Renewable Energy and Power Quality Journal
https://repqj.com/index.php/repqj/index
RE&PQJ, Vol. 23, No. 2, 2025

# Reactive Power Configuration Method for Steady-State Overvoltage in Hydropower Distribution Network Based on Impedance Modulus Margin Index

Yunfeng Yang[1,*],Shutao Hao[1], Duan Zhang[1], Zhangyong Wei[2]

[1]Qinghai Huanghe Hydropower Development Co., Ltd., Xining, 810000, Qinghai Province, China
[2]NR Electric Co., Ltd., Nanjing, 211102, Jiangsu Province, China
[*]Corresponding author's email: bengxingshici8@163.com

**Abstract.** Existing reactive power configuration methods cannot fully consider the impact of dynamic changes in grid topology and load fluctuations when evaluating impedance characteristics and voltage margin, making it difficult to achieve precise regulation in steady-state overvoltage control. To address this issue, this paper constructs a simulation model based on digital twins to simulate the operation status of the power grid in real-time and calculate the impedance modulus margin (IMM) index of each node to precisely evaluate the voltage stability. Then, the grid topology is modeled by graph neural network (GNN); the voltage stability information and reactive power demand between nodes are extracted; the key nodes are identified based on this information. Finally, the PPO (Proximal Policy Optimization) algorithm is utilized to optimize the configuration of reactive power compensation equipment and determine its optimal layout and operation strategy. The experimental outcomes demonstrate that the system voltage stability margin reaches 0.35 in the scenario of multi-equipment collaborative work, and the steady-state overvoltage amplitude is limited to 1.02 times the rated voltage. The research results demonstrate the importance of the IMM-based reactive power configuration method proposed in this paper to enhance the security and voltage stability of hydropower distribution networks.

**Keywords.** Power Grid Stability, Voltage Stability Control, Reactive Power Optimization, Impedance Modulus Margin, Reinforcement Learning Algorithm

## 1. Introduction

Hydropower distribution network is an essential part of the power system and plays a key role in ensuring power supply, optimizing energy utilization, and promoting the development of smart grid. With the gradual replacement of traditional energy by renewable energy [1] and the complexity of power grid structure [2,3], hydropower distribution network [4,5] faces greater challenges in steady-state overvoltage [6] control. Overvoltage [7,8] affects equipment [9,10], causes grid failure [11,12], triggers large-scale power outages, and threatens the safe operation of power system [13,14]. In steady-state overvoltage control, impedance characteristics [15] and reactive power [16,17] configuration play a key role, but traditional reactive power configuration methods ignore the dynamic characteristics of the grid and voltage margin, making it difficult to effectively suppress overvoltage. Existing reactive power dispatch methods [18,19] rely on static analysis, ignore node interaction and nonlinear changes in the grid, and increase the difficulty of voltage stability [20,21] evaluation and optimization dispatch. To meet the growing stability requirements of contemporary power systems, traditional dispatch methods are becoming less and less suitable for complex grid conditions. Most methods have poor adaptability to power grid topology and cannot accurately reflect the impact of factors such as load fluctuations and external disturbances on voltage stability. These methods do not make full use of real-time data and intelligent algorithms in the power grid, making them inefficient in dealing with real-time changes and difficult to achieve precise prediction and dynamic adjustment.

In the study of power systems, voltage stability and overvoltage control have always been key technical issues. Kanojia [22] et al. conducted in-depth research on the application value of voltage stability index in renewable energy-dominated power systems and pointed out that various voltage stability indexes can provide important references for evaluating and optimizing system voltage stability. The application of data-driven methods in power systems has significantly improved the accuracy and adaptability of voltage control strategies [23,24] through real-time data analysis and optimization algorithms. Liu [25] et al. used a data-driven approach to design an adaptive transient overvoltage control strategy for wind farms, which effectively suppressed transient overvoltages in wind farms during grid faults and ensured the stable operation of wind farms. With the

continuous development of power system control methods, new computing technologies have begun to be applied into voltage stability analysis [26,27]. These technologies improve the efficiency of stability analysis and enhance the adaptability to complex system behaviors. Omi [28] et al. proposed a voltage stability margin (VSM) calculation method based on OPF-DM (Optimal-Power-Flow-based Direct Method) and verified it on multiple power system models, proving that it has significantly improved the calculation stability and accuracy compared with traditional methods. These studies have made some progress in voltage stability and overvoltage control [29,30], but there are still problems with insufficient precision and real-time performance in practical applications, especially the integrated application in complex systems has not been fully explored.

In the study of reactive power configuration methods for power grids, different researchers have proposed a variety of effective strategies for improving steady-state overvoltage control and optimizing reactive power distribution. Eid [31] et al. utilized the Improved Marine Predators Algorithm (IMPA) to optimize the optimal configuration of distributed generation and parallel capacitors in the distribution network, effectively reducing the active and reactive power losses of the system and improving voltage stability and overall system performance. As the demand for reactive power compensation in power systems is increasing, researchers have started to concern about how to achieve more efficient reactive power management through advanced scheduling methods [32,33]. Hao [34] et al. proposed a distributed reactive power compensation method using reversible substations in direct-current traction power supply systems, which significantly improved the system power factor and met the need for expensive additional equipment. For different power system network structures, how to accurately estimate and allocate reactive power in the optimal configuration [35,36] has become a key issue in improving system operation efficiency. Therefore, the use of advanced methods based on network topology characteristics has gradually become an effective research direction. Alayande [37] et al. proposed the Network Structural Characteristics Theory (NSCT) and the Network Structure Coefficient Matrix (NSCM) to efficiently estimate and reasonably allocate reactive power losses in interconnected power systems, revealing that the methods based on network topology characteristics have significantly improved the computational complexity and accuracy compared with traditional methods. These methods have achieved certain results in reactive configuration optimization [38,39], but they still have shortcomings in computational complexity, precision control, and adaptability to large-scale power grids.

Hydropower distribution networks face greater challenges in voltage stability as renewable energy sources gradually replace traditional energy sources. With the increasing complexity of the grid structure, steady-state overvoltage control in hydropower distribution networks becomes particularly critical. Traditional reactive power configuration methods make it difficult to accurately assess the impedance characteristics and voltage margin of the grid, and cannot effectively suppress overvoltage phenomena. The method proposed in this study builds a simulation model of a hydropower distribution network based on digital twin technology, accurately assesses voltage stability by calculating the IMM index of each node, and identifies potential overvoltage risks. By constructing a hydropower distribution network simulation model based on digital twin technology, the IMM index of each node is calculated in real-time. The voltage stability of the power grid is precisely evaluated, and potential overvoltage risks are identified. Then, GNN (graph neural network) is used to model the power grid topology, extract the relationship between power grid nodes, and identify key nodes and their reactive power demand. Based on traditional power grid analysis, this paper applies a new data-driven method, which makes full use of the topological structure and operation data of the power grid to realize precise identification of reactive power demand nodes. Then, the reactive power optimization problem is modeled as a multi-dimensional decision-making problem through the PPO (Proximal Policy Optimization) algorithm, and the optimal reactive power compensation strategy is explored under the complex operating conditions of the power grid. By dynamically adjusting the layout and operation of reactive equipment, the power grid can be adjusted in real-time under different load conditions to meet the voltage stability requirements. Through the combination of these technologies, the method proposed in this paper effectively avoids the steady-state overvoltage phenomenon under complex power grid conditions, and also improves the adaptive ability and stability of the power grid. The method adopted in this paper successfully controls the overvoltage amplitude under multiple operating conditions and significantly improves the voltage stability margin of the power grid, providing a new solution for the reactive power optimization of hydropower distribution networks.

## 2. Reactive Power Optimization Methods

### *A. Construction of Hydropower Distribution Network Simulation Model*

The hydropower distribution network simulation model is based on digital twin technology and realizes high-precision simulation of the grid operation status through a comprehensive construction process. The construction of the model is centered on the topological structure of the grid. First, it is necessary to obtain complete distribution network operation data, which includes key parameters such as node voltage state, impedance characteristics, and power distribution. Then, these data are used to generate a node-edge topology graph, where nodes represent substations or load centers in the grid and edges represent electrical connections between nodes. By analyzing the topological relationship and electrical parameters, a mathematical model

reflecting the actual characteristics of the grid is constructed.

The simulation model is based on the node admittance matrix $Y$ to describe the impedance characteristics between nodes. The elements of the node admittance matrix are defined by Formula (1):

$$Y_{ij} = \begin{cases} \sum_{k \neq 1} Y_{ik}, if\ i = j \\ -Y_{ij}, if\ i \neq j \end{cases} \quad (1)$$

In formula (1), $Y_{ij}$ is the admittance value between nodes $i$ and $j$. The precise construction of the admittance matrix ensures that the model precisely describes the impedance characteristics of the grid. The simulation model needs to dynamically simulate the operation state of the power grid. Its core is to calculate the voltage and power distribution of the node through the power balance equation:

$$P_i = V_i \sum_{j=1}^{n} V_j (G_{ij} \cos\theta_{ij} + B_{ij} \sin\theta_{ij}) \quad (2)$$

$$Q_i = V_i \sum_{j=1}^{n} V_j (G_{ij} \sin\theta_{ij} + B_{ij} \cos\theta_{ij}) \quad (3)$$

In formula (2) and (3), $P_i$ and $Q_i$ are the active power and reactive power of node $i$ respectively; $V_i$ and $V_j$ are the node voltage amplitudes; $G_{ij}$ and $B_{ij}$ are the real and imaginary parts of the admittance; $\theta_{ij}$ is the phase difference between nodes.

To further enhance the adaptability of the simulation model, this paper applies a load dynamic characteristic model to describe the change law of the load under different voltage conditions. The model adopts the following forms:

$$P_L = P_0 \left( \frac{V}{V_0} \right)^a \quad (4)$$

$$Q_L = Q_0 \left( \frac{V}{V_0} \right)^b \quad (5)$$

In formula (4) and (5), $P_0$ and $Q_0$ are rated loads; $V_0$ is rated voltage; $a$ and $b$ are load indexes, which reflect the sensitivity of voltage to active and reactive loads respectively.

### *B. Calculation of IMM Index*

The IMM index is a key indicator for measuring the voltage stability of each node in the power grid. Its core lies in calculating the ratio of node impedance to critical impedance. This ratio reflects the ability of each node in the power grid to withstand voltage fluctuations without instability. The higher the IMM value, the more stable the node voltage; conversely, there is a higher risk of voltage instability. The dynamic update of the IMM combines the changes in node state variables and the admittance matrix Y under different operating conditions to ensure an accurate assessment of the real-time voltage stability of the power grid. The calculation of IMM index is based on the grid state parameters generated by the simulation model and is used to evaluate the voltage stability of each node. The core of the IMM index is to calculate the ratio between the impedance modulus of the node and its critical value. Assuming that the equivalent impedance of node $i$ is $Z_i$, the equivalent impedance of the node is calculated by the inverse matrix $Z = Y^{-1}$ of the node admittance matrix $Y$. The self-impedance $Z_{ii}$ of node $i$ is:

$$Z_{ii} = \frac{1}{Y_{ii}} \quad (6)$$

If there is an electrical connection between node $i$ and other node $j$, its equivalent impedance needs to comprehensively consider the connection relationship and is calculated by the following equation:

$$Z_{eq,i}(t) = Z_{ii}(t) + \sum_{j \in N_i} T_{ij}(t) \cdot Z_{ij}(t) \quad (7)$$

In formula (6) and (7), $Z_{ij}$ is the coupling impedance between nodes $i$ and $j$. $T_{ij}(t)$ is the topology change matrix, which reflects the dynamic adjustment of the connection status between nodes after a fault occurs.

The critical impedance is determined by the voltage stability margin of the node and reflects the maximum impedance value that the node can withstand before instability. For a given node $i$, the critical impedance $Z_{i,\text{crit}}$ is calculated as follows:

$$Z_{i,\text{crit}} = \frac{V_i^2}{S_i} \quad (8)$$

$V_i$ is the nominal voltage of the node, and $S_i$ is the apparent power of the node.

The IMM index is defined as the ratio of the equivalent impedance modulus value of the node to the critical impedance modulus value, and the equation is:

$$\text{IMI}_i = 1 - \frac{|Z_i|}{|Z_{i,\text{crit}}|} \quad (9)$$

$\mathrm{IMI}_i$ is the IMM of node $i$.

To ensure the dynamic adaptability of the index, the IMM needs to be calculated in combination with different operating conditions. When the load changes or the topology is adjusted, the voltage and power state of the node changes, thereby affecting the equivalent impedance value and the critical impedance value. The IMM index is dynamically updated by real-time monitoring of the node state variables $V_i$ and $S_i$ and the admittance matrix $Y$:

$$\mathrm{IMI}_i = 1 - \frac{\sum_{j=1}^{n} |Z_{ij}|}{Z_{i,\mathrm{crit}}} \quad (10)$$

The calculation result of the IMM can intuitively reflect the voltage margin of the node and provide an important reference for identifying key nodes in the power grid.

### C. GNN Modeling of Power Grid Topology Characteristics

GNN modeling of power grid topology characteristics aims to construct adjacency matrix and node feature matrix based on the topological structure and node characteristics of the power grid, and to describe the operation status of the power grid in mathematical form. Through GNN layer-by-layer information aggregation, the correlation characteristics between nodes and neighboring nodes are extracted to achieve accurate prediction of node voltage stability requirements, providing precise support for IMM analysis and reactive power compensation optimization configuration. The construction and training process of the GNN model is illustrated in Figure 1.

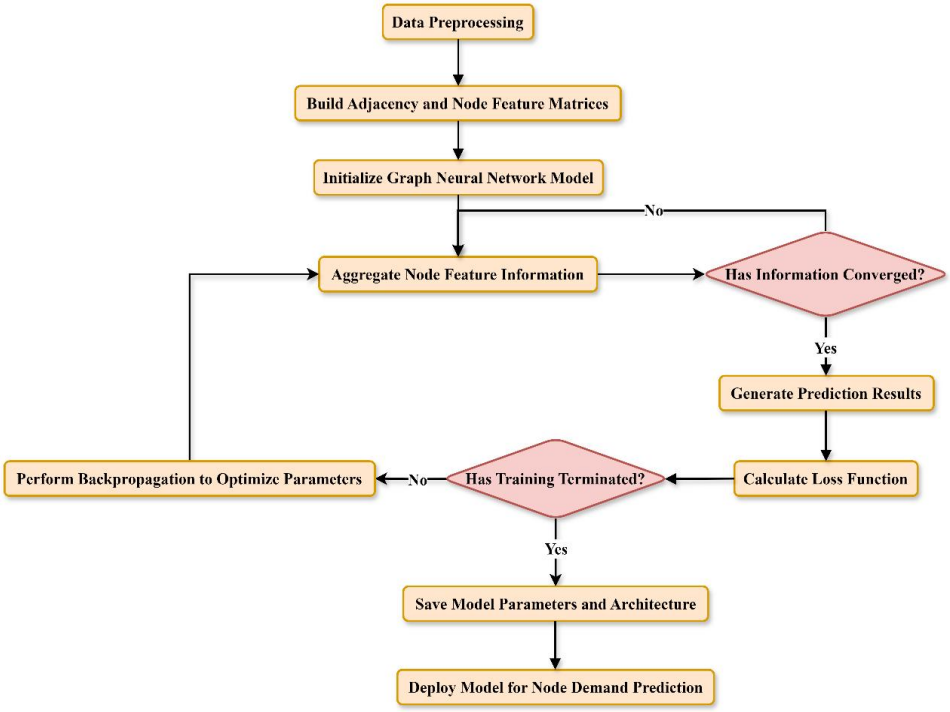


Figure 1. Model construction and training.

In the process of model construction, the digital twin simulation model is first used to generate power grid topology data, including the adjacency matrix $A$ and the node feature matrix $X$. $A$ represents the power grid topology structure, and its element $A_{ij}$ is the indicator value of whether nodes $i$. and $j$ are connected. The node feature matrix $X$ is:

$$X = \begin{bmatrix} V_1, & \theta_1, & Q_1 \\ V_2, & \theta_2, & Q_2 \\ \vdots & \vdots & \vdots \\ V_n, & \theta_n, & Q_n \end{bmatrix} \quad (11)$$

The construction of GNN follows the idea of information aggregation to capture the electrical characteristics and topological influences between nodes. Its core is to update the feature representation $H^{(l)}$ of the node layer by layer, and gradually refine the implicit relationship of power grid voltage stability by integrating the information of neighboring nodes. In the lth layer, thepdate equation of node features is:

$$H_i^{(l+1)} = \sigma\left( \sum_{j \in \mathcal{N}(i)} \frac{1}{\sqrt{d_i d_j}} A_{ij} H_j^{(l)} W^{(l)} + b^{(l)} \right) \quad (12)$$

$\mathcal{N}(i)$ is the set of neighbor nodes of node $i$; $d_i$ is the degree of node $i$; $W^{(l)}$ and $b^{(l)}$ are trainable weights and biases.

The final output of the network is the voltage stability demand prediction value of the node. This paper uses a multi-layer perceptron (MLP) to map implicit features to specific requirements:

$$Y_i = \text{Softmax}(W_{\text{out}} H_i^{(L)} + b_{\text{out}}) \quad (13)$$

$W_{\text{out}}$ and $b_{\text{out}}$ are output layer parameters, and $H_i^{(L)}$ is the node implicit feature extracted from the Lth layer. The predicted value $Y_i$ is used to describe the reactive power demand of the node under different operating conditions.

To ensure the efficiency and accuracy of the model training and testing phases, this paper uses the historical data output by the digital twin simulation model to train the GNN. The objective function uses the cross entropy loss:

$$\mathcal{L} = -\frac{1}{n}\sum_{i=1}^{n}\sum_{c=1}^{C} y_{i,c} \log \hat{y}_{i,c} \quad (14)$$

In formula (14), $C$ is the predicted classification number, and $y_{i,c}$ and $\hat{y}_{i,c}$ represent the actual category label and predicted probability of node $i$, respectively. Through the back propagation algorithm, parameters such as $W^{(l)}$, $b^{(l)}$, $W_{\text{out}}$, and $b_{\text{out}}$ are optimized. After model training, in actual deployment, the GNN model is used to quickly predict the voltage stability requirements of each node in the power grid through real-time updates of power grid operation data, thereby providing efficient support for IMM index calculation and reactive equipment optimization.

### *D. Reactive Compensation Equipment Optimization*

The reactive compensation equipment optimization is based on the calculation results of the IMM index and the node reactive demand, combined with the grid characteristics predicted by the GNN model and the strategy search of the reinforcement learning algorithm, aiming to achieve the optimal reactive compensation layout and operation mode, and ensure the stability and safety of the grid operation. The IMM index reflects the stability margin of the node voltage, and the reactive demand reflects the distribution characteristics of the electrical load of each node. The two serve as the core information sources of the optimization process. The optimization process of the reactive compensation equipment revolves around the IMM analysis and the node reactive demand prediction. The strategy optimization and layout adjustment are completed through algorithm iteration, and finally, a compensation scheme that meets the grid operation requirements is generated. Figure 2 describes the complete optimization process.

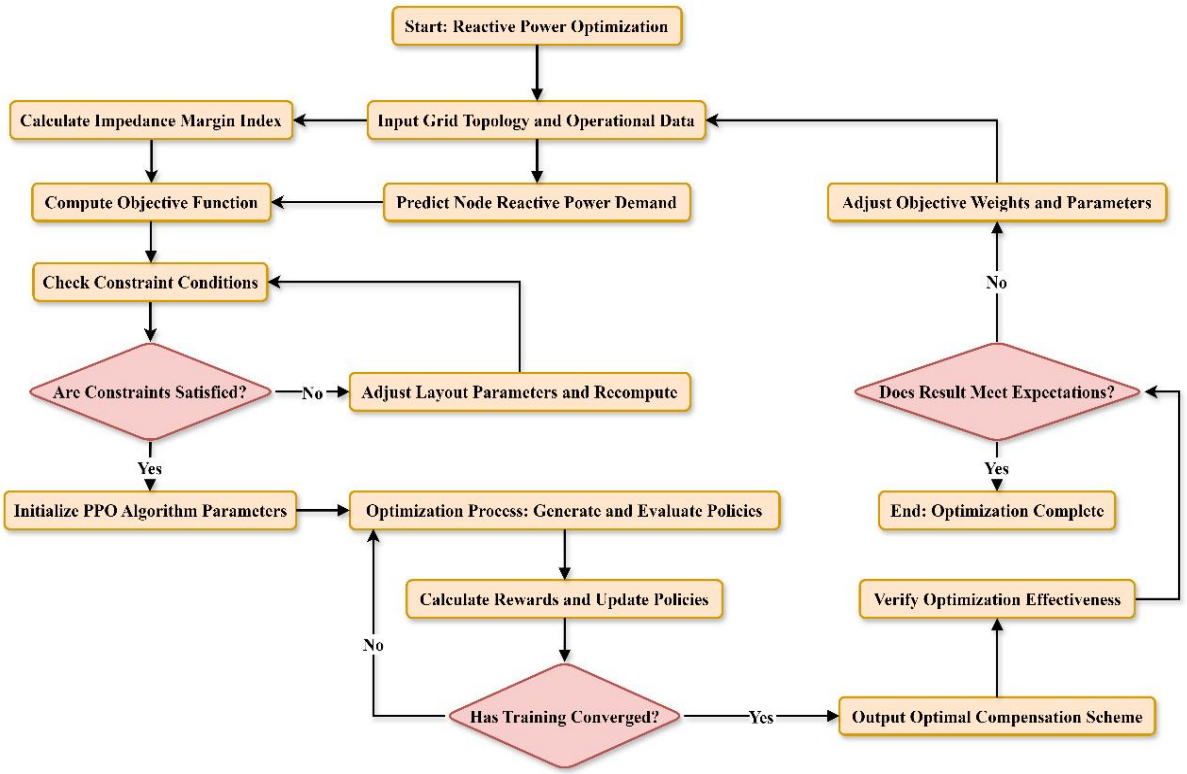


Figure 2. Reactive power compensation equipment optimization process.

The reactive power compensation optimization problem aims to maximize voltage stability and reactive power demand satisfaction. The optimization direction is characterized by applying a weighted comprehensive objective function. The optimization process defines the objective function as follows:

$$\max_{\mathbf{P}} J = \sum_{i=1}^{n} (w_1 \cdot \mathrm{IMI}_i + w_2 \cdot Y_i) \quad (15)$$

In formula (15), $\mathbf{P}$ is the layout parameter, and $w_1$ and $w_2$ are weights that measure the relative importance of IMM and reactive power demand. The optimization problem is subject to multiple constraints, among which the total capacity of the reactive power compensation equipment, the node voltage range, and the power transmission capacity of the power grid are as follows:

$$\sum_{i=1}^{m} Q_{o,i} \le Q_{max} \quad (16)$$

$$V_{min} \le V_i \le V_{max}, \forall i \in \mathcal{N} \quad (17)$$

$$P_{ij}^2 + Q_{ij}^2 \le S_{ij}^2, \forall (i,j) \in \mathcal{E} \quad (18)$$

$Q_{o,i}$ is the reactive power compensation equipment output at the node; $Q_{max}$ is the total equipment capacity limit; $P_{ij}$ and $Q_{ij}$ are the active and reactive power on the line, respectively; $S_{ij}$ is the line power capacity; $\mathcal{N}$ and $\mathcal{E}$ are the node set and edge set, respectively.

The PPO algorithm is applied in the optimization process, combined with the reinforcement learning method to search for the optimal reactive power compensation layout and operation strategy. This method takes the IMM, voltage state, and reactive power distribution as state inputs, and optimizes the adjustment of layout parameters as action outputs. The strategy iteration process achieves the system optimization direction by maximizing the cumulative reward. The reward function is defined as the increment of the objective function:

$$R = \Delta F - \lambda_1 C_{act} - \lambda_2 P_{volt} \quad (19)$$

In formula (19), $R$ is the modified reward value, $\Delta F$ represents the increment of the objective function, $C_{act}$ is the cost incurred by equipment activation, $P_{volt}$ is the penalty introduced by voltage exceeding the limit, and $\lambda_1$ and $\lambda_2$ are weight coefficients used to balance the relative importance of the optimization objective and the penalty term.

By calculating the change of the reward value, the reinforcement learning agent is guided to adjust the equipment layout parameters in the dynamic power grid condition, so that the overall system is more inclined to the optimal voltage stability and reactive power demand satisfaction effect. The PPO algorithm ensures the stability of optimization by limiting the amplitude of the strategy update. Its update target is:

$$\max_{\theta} \mathbb{E}_t \left[ min(r_t(\theta)\hat{A}_t, \mathrm{clip}(r_t(\theta), 1-\ , 1+\ )\hat{A}_t) \right] \quad (20)$$

In formula (20), $\theta$ is the strategy parameter; $r_t(\theta)$ is the probability ratio of the current strategy to the old strategy; $\hat{A}_t$ is the advantage function; $\epsilon$ is the shear boundary. This process gradually adjusts the reactive compensation equipment layout and output strategy under the constraints, so as to ensure that the final layout can meet the needs of different operating conditions.

In the process of implementing GNN model training and PPO algorithm optimization, the computational cost is mainly reflected in the feature extraction of large-scale topological data and the policy iterative search in the high-dimensional state space. The GNN model encodes the complex relationship between power grid nodes through multi-layer information aggregation, and this process requires multiple matrix operations on the adjacency matrix and the node feature matrix. As the scale of the power grid increases, the dimension and sparsity of the matrix have an increasingly significant impact on the computing time. Especially in the digital twin environment with high-frequency dynamic feature updates, the time complexity of model training shows a nonlinear growth. The PPO algorithm needs to perform multiple rounds of iterations in the policy space to guide the policy update through the convergence objective function, and each round of optimization involves a large number of sample evaluations and gradient calculations. In order to ensure the convergence speed and model stability, PPO adopts policy clipping and discounted reward mechanisms to further improve the computational intensity. In response to the above problems, the experiment deployed high-performance hardware resources, and by adjusting the model hyperparameters and optimization step size, the computational overhead was effectively reduced while improving the algorithm effect. When dealing with larger-scale power grid topologies or complex fault scenarios, existing computing resources will become a key factor limiting its real-time and universality. How to reduce the computational cost while ensuring the optimization performance is an important direction for future research.

## 3. Experimental Design and Implementation

### *A. Experimental Dataset and Scenario Design*

The experimental data set is derived from the historical operation records of the regional power grid of a hydropower development company, covering real-time monitoring data from 2020 to 2023. The scale of the power grid involved in the data set is 120 nodes, covering industrial, commercial, residential and transmission nodes, of which industrial nodes account for 29.2%, commercial nodes account for 20.8%, residential nodes account for 33.3%, and transmission nodes account for 16.7%. The penetration rate of renewable energy reaches 48%, mainly including

hydropower and wind power, reflecting the energy structure characteristics of the current regional power grid. The load fluctuation range is between ±15% and ±35%, showing dynamic changes under different time periods and load conditions. Fault frequency statistics show that the average annual fault rate is 2.1%, among which single-line faults and high-voltage equipment faults are the most common, accounting for 56% and 31% of the total faults, respectively.

The verification of the digital twin model ensures the accuracy and reliability of the model under different working conditions by comparing the simulation results with the actual power grid operation data. The model's ability to describe the dynamic characteristics of the power grid is verified by matching the simulation results of node voltage, reactive power distribution, and power grid topology changes with actual monitoring data. In terms of error analysis, the root mean square error (RMSE) is used to evaluate the difference between the simulation data and the actual power grid data. The experimental results show that the RMSE of the node voltage is 0.024 pu and the RMSE of the reactive power distribution is 1.8 MVAr, indicating that the digital twin model has high accuracy in simulating the steady-state and dynamic characteristics of the power grid. Through the above verification and error analysis, the effectiveness of the proposed method and the credibility of the results are ensured.

The experimental data is strictly cleaned and preprocessed before use to ensure the accuracy and reliability of the experimental results. The data cleaning process deals with missing values, outliers, and redundant information in the original data. For missing values, combined with the time series characteristics of the data, interpolation and historical data regression prediction methods are used to supplement them to ensure the integrity of the data. Regarding outlier detection, the triple standard deviation rule based on statistical methods and the isolation forest algorithm based on machine learning are used to identify outliers in the data, and the voltage, load, and impedance parameter values that exceed the reasonable range are marked and eliminated. For redundant information, feature selection technology is used to remove data features that do not contribute to the experimental analysis or have low relevance to reduce data complexity and computing resource consumption. The preprocessing process is carried out on the basis of the cleaned data, mainly including normalization and feature conversion. Normalization processing uniformly scales the voltage, load, and impedance parameters of the power grid operation data to the same numerical range. Feature transformation extracts the main features of the data through principal component analysis (PCA) and factor analysis, compresses the data dimension, enhances the sensitivity of the model to key parameters, and avoids the interference of redundant features on the model performance. Data time alignment is also a key step in preprocessing. All operating data are synchronized according to a unified timestamp to ensure that the status information of different equipment can be accurately analyzed under the same time reference.

To analyze the impact of different types of nodes on the steady-state overvoltage of the power grid and their characteristics, industrial, commercial, residential, and transmission nodes are classified and summarized based on experimental data, and key statistical parameters are extracted, as described in Table 1.

Table 1. Node type and characteristic statistics.

| Node Type | Node Count | Average Node Voltage (kV) | Average Active Power (MW) | Average Reactive Power (MVAr) | Average Voltage Margin | Steady-State Overvoltage Occurrence (%) |
|---|---|---|---|---|---|---|
| Industrial Nodes | 35 | 11.5 | 6.2 | 2 | 0.94 | 3.8 |
| Commercial Nodes | 25 | 10.7 | 5.8 | 1.9 | 0.91 | 4.5 |
| Residential Nodes | 40 | 11.1 | 4.5 | 1.6 | 0.92 | 4 |
| Transmission Nodes | 20 | 12 | -- | -- | 0.95 | 2.7 |

Table 1 shows the main power characteristics and steady-state overvoltage related indicators of different types of nodes. By statistically analyzing the voltage, power, reactive power demand, and voltage margin of industrial, commercial, residential, and transmission nodes, the performance of various types of nodes in the steady-state operation of the power grid is understood, providing crucial basic data support for the subsequent reactive power optimization analysis and voltage stability assessment. The voltage margin value is obtained by calculating the ratio of the impedance modulus of each node to its critical value. It is specifically based on the grid state parameters generated by the digital twin simulation model and is updated in real time under different load changes and topology adjustment conditions to reflect the voltage stability of the node.

The simulation model is expanded according to the operating characteristics of the real power grid, supplemented with a variety of operating conditions and equipment configurations, covering different states such as normal operation, load fluctuation, and fault occurrence to simulate the complex situations in the actual scenario. The design of the experimental scenario builds a dynamic simulation environment based on

digital twin technology to ensure that the dynamic characteristics of the power grid under various operating conditions can be reflected in real-time. In the scenario design, the typical operating conditions of the hydropower distribution network are selected as the test basis, and a variety of load change curves are set to evaluate the impact of load fluctuations on the stability of the power grid. In the experiment, line disconnection, equipment maintenance, and other situations are also set to simulate the steady-state characteristics of the power grid under different topological conditions. The study of the steady-state overvoltage problem needs to focus on the situation where the node voltage deviates from the rated value. Therefore, different reactive power demand distribution modes are designed in the simulation environment to analyze the impact of reactive power distribution on voltage stability. The experimental data and scenarios are based on the premise of supporting multiple repeated experiments to ensure the standardization of data input and the verifiability of experimental results under different configuration conditions. In this way, the experimental data and scenario design lay a solid foundation for subsequent reactive power optimization analysis and method verification.

### *B. Experimental Parameter Configuration and Model Implementation*

To ensure the accuracy and repeatability of simulation results, this paper builds a high-performance hardware and software environment, including computing resources and simulation and deep learning frameworks to meet the computing requirements of digital twin simulation and model training. Table 2 lists the hardware and software configurations used in this experiment.

This paper sets initial parameters for the GNN model and PPO algorithm respectively, and adjusts them during the experiment to obtain a better reactive compensation configuration effect. Table 3 shows the initial values, adjustment ranges, and final optimization results of each key parameter in the experiment.

Table 2. Experimental environment configuration table.

| Category | Name | Model/Version | Quantity |
|---|---|---|---|
| Hardware | CPU | Intel Core i5-13600K | 1 |
| | GPU | NVIDIA RTX 4060 | 1 |
| | Memory | 8GB DDR4 | 4 |
| | Storage Equipment | 4TB SSD | 4 |
| Software | Operating System | Windows 10 | 1 |
| | Simulation Platform | MATLAB/Simulink R2021a | 1 |
| | Deep Learning Framework | TensorFlow 2.8.0 | 1 |
| | Reinforcement Learning Framework | Stable-Baselines3 1.5.0 | 1 |
| | Programming Language & Tools | Python 3.9 | 1 |

Table 3. Experimental parameter setting table.

| Parameter Name | Initial Value | Adjustment Range | Optimized Value |
|---|---|---|---|
| Impedance Margin Step | 0.01 pu | 0.005-0.02 | 0.008 pu |
| GNN Layers | 3 | 2-5 | 4 |
| GNN Hidden Layer Dimension | 128 | 64-256 | 192 |
| GNN Learning Rate | 0.001 | 0.0005-0.01 | 0.0008 |
| PPO Discount Factor | 0.99 | 0.9-1.0 | 0.97 |
| PPO Learning Rate | 0.0003 | 0.0001-0.001 | 0.00025 |
| PPO Training Episodes | 10000 | 5000-20000 | 15000 |
| PPO Batch Size | 64 | 32-128 | 96 |
| Reinforcement Learning Steps | 100000 | 50000-200000 | 150000 |
| Digital Twin Simulation Step | 1s | 0.5s-2s | 1.2s |
| Voltage Stability Margin Threshold | 0.35 | 0.3-0.5 | 0.38 |
| Overvoltage Control Limit | 1.1 pu | 1.05-1.2 pu | 1.08 pu |

The hyperparameters involved in the PPO algorithm have a direct impact on training stability and convergence characteristics. The learning rate determines the amplitude of parameter updates and affects the convergence speed and stability. A higher learning rate speeds up convergence but causes policy oscillations, while a lower learning rate enhances stability but increases training time. The discount factor affects the importance of future rewards in the decision-making process. A larger discount factor helps optimize long-term returns, while a smaller discount factor enhances adaptability to short-term changes. The batch size affects the statistical reliability of gradient estimation. A larger batch size reduces the gradient variance and improves the stability of policy updates, but increases computational overhead. A smaller batch size increases the frequency of policy updates and introduces higher volatility. These hyperparameters determine how

the PPO algorithm explores and utilizes the search space during the optimization process, affecting the balance between computational cost and optimization effect.

## 4. Results

### *A. Relationship between IMM Index and Voltage Stability*

This paper experimentally constructs a simulation platform based on digital twin technology, comprehensively simulates the dynamic behavior of hydropower distribution network under various operating conditions, and uses IMM index to quantify voltage stability characteristics. The experiment aims to provide a scientific basis for optimizing reactive power configuration by precisely evaluating the impedance distribution characteristics under different load levels and operating conditions. According to the calculation results of IMM, the experiment further analyzes its influence on the steady-state overvoltage of the power grid in combination with various load levels and operating conditions, and summarizes its changing characteristics under different scenarios. The outcomes are displayed in Figure 3.

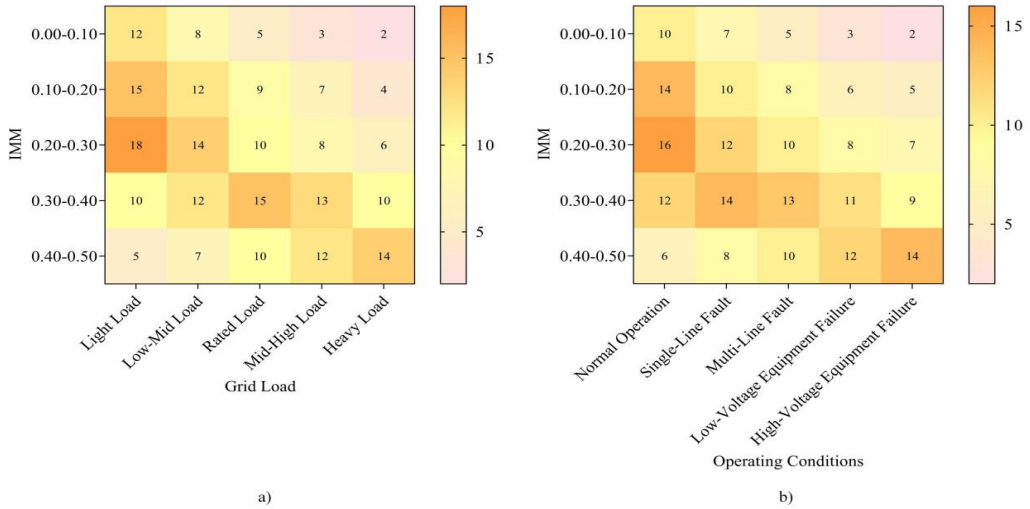


Figure 3. Relationship between IMM and power grid operating characteristics. (a) Analysis of IMM indicators and different grid loads; (b) Analysis of different operating conditions.

The data points in Figure 3 represent the distribution of the IMM index of each node in the power grid under different load levels and operating conditions. Under light load and medium-low load conditions, the IMM is mainly distributed in the range of 0.20-0.30, showing a stable characteristic. As the load gradually increases, the IMM shifts to a higher range. Among them, under heavy load conditions, the proportion of the 0.30-0.40 interval increases significantly, indicating that as the load increases, the system voltage stability gradually weakens. Combined with the reactive power demand characteristics of the power grid, the increase in reactive power demand under higher load conditions leads to a decrease in voltage margin, which in turn causes the risk of voltage instability. The analysis results of operating conditions further reveal the impact of different operating conditions on the distribution of IMM. Under normal operating conditions, the IMM is mainly distributed in the 0.20-0.30 interval. Under abnormal conditions such as single line faults and high-voltage equipment failures, the distribution of IMM is obviously biased towards the high interval, and some nodes are concentrated in the 0.30-0.40 interval or even higher. This distribution change indicates that abnormal conditions significantly weaken the voltage stability of the system, which is related to the change in power grid topology and the decrease in reactive compensation capacity under fault conditions. These data show that different operating conditions have a profound impact on the distribution characteristics of IMM, and strengthening the reactive power optimization strategy under operating conditions is a key measure to ensure voltage stability.

The IMM index reflects the ratio of the node impedance modulus to its critical value, and directly indicates the stability margin of the node voltage. A higher IMM value means that the node is closer to an unstable state and the voltage stability decreases. When the load increases, the equivalent impedance of the node increases, resulting in an increase in the IMM value, a decrease in the voltage margin, and a greater tendency for the system to experience voltage instability. Under different operating conditions, changes in the grid topology and reactive power distribution will change the electrical coupling relationship between nodes, thereby affecting the ratio of equivalent impedance to critical impedance, leading to fluctuations in the IMM index. When operating conditions are abnormal, situations such as single-line faults and equipment failures will significantly increase the IMM values of some nodes, causing local voltage instability. This mechanism shows that the voltage stability of the power grid is highly dependent on the dynamic balance between the impedance characteristics of the node and the load level, and the IMM index provides a reliable basis for identifying key

nodes and optimizing reactive power configuration.

### *B. Impact of Reactive Power Compensation Strategy on Overvoltage Control*

Five typical scenarios are set up in the experiment. Conditions 1 to 5 are light load, medium-light load, medium load, medium-heavy load, and heavy load, respectively, to simulate the operating status of the real power grid and its potential challenges. Under light load conditions, the overall load of the power grid is low, and the voltage level is relatively stable. In medium-light load conditions, load fluctuations are applied to examine the adaptability of reactive power optimization to dynamic load changes. In medium load conditions, the maintenance conditions of key reactive power compensation equipment are simulated to test the effect of the optimization strategy when the equipment is out of service. Medium-heavy load conditions apply complex scenarios of line disconnection to evaluate the steady-state characteristics under topology changes. Heavy load conditions combine high load operation with equipment failure. The performance of the PPO algorithm-based method is compared with the reactive power dispatching method based on traditional optimal power flow (OPF) and the improved PSO (Particle Swarm Optimization) algorithm. The experiment takes the steady-state overvoltage amplitude and IMM as the core indicators. The outcomes are displayed in Figure 4.

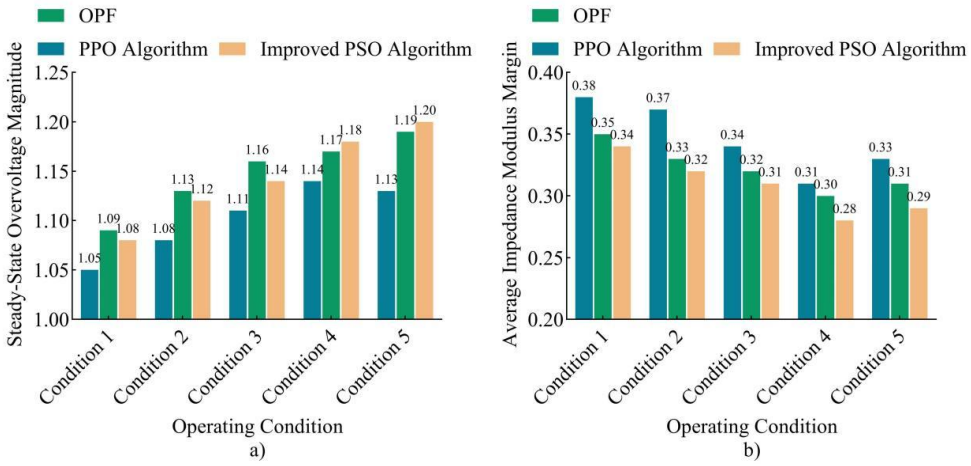


Figure 4. Comparison of reactive power optimization methods under different operating conditions. (a) Steady-state overvoltage amplitude comparison; (b) IMM comparison.

The data points in Figure 4 represent the steady-state overvoltage amplitude and average IMM index of different optimization methods under different load conditions. In heavy load conditions, the PPO algorithm controls the overvoltage amplitude at 1.13 times the rated voltage, while the OPF and the improved PSO algorithm reach 1.19 times and 1.20 times, respectively, showing that the latter two methods are insufficient in coping with high loads and complex topologies. In terms of IMM, the PPO algorithm reaches 0.37 under medium-light load conditions and maintains at 0.33 under heavy load conditions, while the OPF is 0.33 and 0.31, respectively, reflecting the trend that its optimization effect gradually weakens with the increase of load. This result shows that the PPO algorithm is more effective in dynamically adjusting the reactive compensation strategy and has higher adaptability and stability to complex operating conditions. The strategy optimization of the PPO algorithm relies on the node features extracted by GNN. Key nodes are preferentially identified by their high impedance modulus margin and reactive power demand, and compensation equipment configuration prioritizes these nodes to maximize the voltage stability of the power grid and reduce the risk of overvoltage.

### *C. Influence of Grid Topology on Reactive Configuration Effect*

In reactive configuration optimization, the characteristics of different grid topologies directly affect the performance of voltage stability margin and overvoltage amplitude. The radial topology is prone to voltage fluctuations at key nodes due to its single power transmission path. The ring topology has good power dispersion capabilities, but the reactive power demand between nodes is easily affected by the loop flow. The grid topology can improve system redundancy and stability due to its multi-path power transmission mechanism. The star topology has a greater risk of voltage fluctuations under the structure of centralized power supply. Although the tree topology has the advantage of hierarchical distribution, the voltage stability of its edge nodes is poor when the load changes greatly. Based on these characteristics, an experiment is constructed to compare the specific effects of different power grid topologies in reactive power configuration optimization, and analyze their effects on voltage stability margin and steady-state overvoltage amplitude. Figure 5 summarizes the above experimental results.

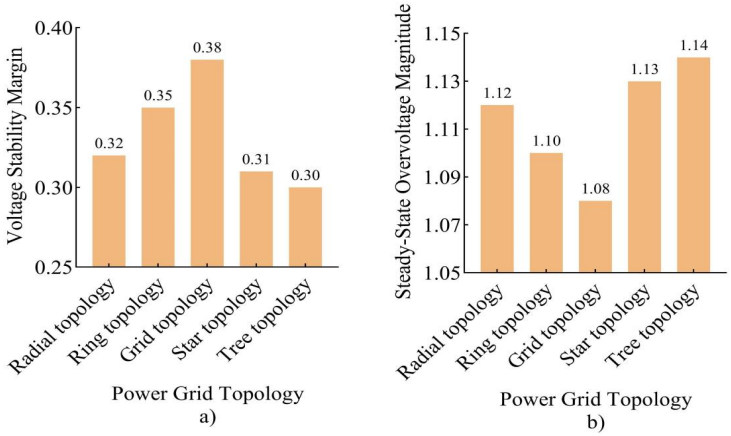


Figure 5. Effects of different power grid topologies on reactive power configuration optimization. (a) Effect of different grid topologies on voltage stability margin; (b) Effect of different grid topologies on overvoltage amplitude.

The data points in Figure 5 represent the voltage stability margin and steady-state overvoltage amplitude under different grid topologies, revealing the impact of topology on reactive power optimization effect. The highest voltage stability margin of 0.38 in the experiment. This is mainly attributed to its multi-path power transmission characteristics, which effectively reduces the voltage fluctuations at key nodes and improves the reactive power distribution efficiency of the system. The voltage stability margin of the ring topology reaches 0.35, and its closed-loop design enhances the stability of the system while reducing reactive power transmission losses. The voltage stability margins of the radial and star topologies are 0.32 and 0.31, respectively. Due to their centralized structures, some nodes become voltage weak points, limiting the stability performance of the system. The voltage stability margin of the tree topology is the lowest, at 0.30, mainly because the hierarchical distribution leads to a significant decrease in the efficiency of reactive power distribution from the central node to the edge node. In terms of steady-state overvoltage amplitude, the grid and ring topologies are 1.08 times the rated voltage and 1.10 times the rated voltage, respectively, showing excellent overvoltage control capabilities. The overvoltage amplitudes of the radial and star topologies are 1.12 times the rated voltage and 1.13 times the rated voltage, respectively, which are higher than the grid and ring topologies. The overvoltage amplitude of the tree topology is the highest, reaching 1.14 times the rated voltage, which is mainly due to the limitations of the tree topology on the power transmission path, resulting in serious voltage accumulation at some nodes. Although grid and ring topologies are excellent in improving voltage stability, their construction and maintenance costs are significantly higher than radial and star topologies. Due to their simple structure and low cost, radial and star topologies still have high economic feasibility in practical applications and are suitable for cost-constrained grid transformation projects. The overall analysis shows that a reasonable design of the power grid topology can significantly improve the optimization effect of reactive configuration.

The power grid topology determines the electrical coupling relationship between the power transmission path and the nodes, thus affecting the voltage stability. The radial structure has a single power transmission path, and some key nodes are prone to become bottlenecks. When the load increases or a fault occurs, the local voltage support capacity drops rapidly. The central node of the star structure undertakes the main power distribution task. Load fluctuations or equipment adjustments directly affect the voltage distribution of the entire system, and the voltage regulation ability of the peripheral nodes is poor. The hierarchical distribution of the tree structure causes the lower nodes to rely on the upper voltage support. Long-distance power transmission causes a large voltage drop, and the end nodes have a higher demand for reactive power compensation. The power transmission path of the ring structure is relatively balanced, but the circulation effect affects the reasonable distribution of reactive power. Voltage deviations occur at specific nodes due to insufficient reactive power compensation. The electrical characteristics of different topologies determine the voltage regulation and fault recovery capabilities of the power grid. Structural limitations directly affect the strength of voltage stability.

### *D. Performance of Reinforcement Learning Algorithm in the Optimization Process*

In the process of reactive power compensation optimization of power grid, the change of model convergence performance directly affects the stability and optimization effect of the system. To deeply explore the performance of PPO algorithm in reactive power compensation configuration, this experiment records the changes of voltage stability margin and convergence rate under different training rounds, and analyzes the convergence trend of the algorithm in multiple iterations

and its impact on power grid stability. This process not only reflects how the PPO algorithm gradually adjusts the configuration of reactive power compensation equipment, but also reveals the stability improvement in the optimization process. On this basis, Figure 6 depicts the convergence analysis of PPO algorithm in reactive power compensation optimization process.

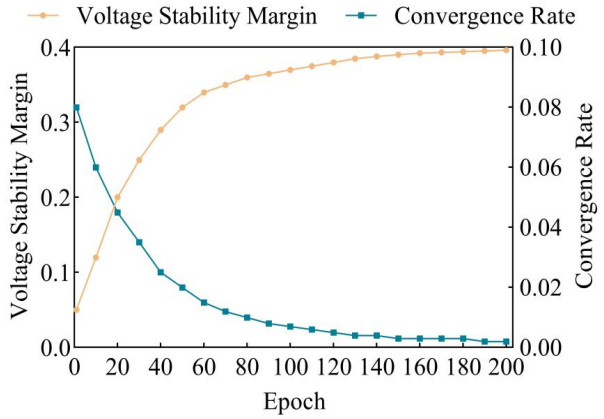


Figure 6. Performance of PPO algorithm in reactive power compensation optimization.

The data points in Figure 6 show the changes in voltage stability margin and convergence rate of the PPO algorithm under different numbers of training rounds, reflecting the trend of the algorithm gradually improving system stability during the optimization process. With the increase of training rounds, the voltage stability margin gradually stabilizes, and the initial growth is relatively rapid. In the 50th round, the voltage stability margin has increased from 0.05 to 0.32, showing the significant optimization effect of the algorithm in the early stage. From the 100th round, the voltage stability margin gradually stabilizes, and the increase gradually slows down and finally tends to 0.396. This stable value reflects the convergence state of the optimization process. The change in convergence rate reflects the gradual stabilization of the algorithm. Starting from the initial 0.080, as the number of training rounds increases, the convergence rate continues to decline, approaching 0.002 at 200 rounds, indicating that after completing a certain number of optimizations, the adjustment speed of the PPO algorithm slows down significantly and enters the convergence stage. These changes show that as the optimization proceeds, the PPO algorithm can stably enhance the voltage stability margin of the power grid and reduce fluctuations during the convergence process, proving that the application of this method in the hydropower distribution network has good stability and effectiveness.

### *E. Optimization Effect of the Method on Steady-State Overvoltage Control of the Power Grid*

In the optimization process of steady-state overvoltage control of the power grid, different operating scenarios have different degrees of impact on the stability of the power grid. The load change scenario mainly simulates the challenge of power grid load fluctuations to voltage stability. Load increases and decreases directly affect the voltage stability margin of the power grid. The line fault scenario simulates the situation of a power grid failure, examines the steady-state overvoltage response of the power grid when a fault occurs, and detects its recovery ability. The multi-equipment collaborative operating scenario focuses on analyzing the impact of multiple reactive compensation equipment on the stability of the power grid under simultaneous action, aiming to verify the synergy between different equipment. The high load and low load switching scenarios evaluate the adaptability and voltage stability of the power grid in load fluctuations by simulating the voltage changes during load switching. The complex topology scenario analyzes the impact of the topology on the optimization of the reactive configuration of the power grid by comparing the performance of the voltage stability margin under different power grid topologies. Through the design of these experimental scenarios, this experiment aims to evaluate the application effect of the optimization method under various actual power grid conditions, and further analyze the improvement effect of the optimization method on the steady-state overvoltage control of the power grid. Figure 7 illustrates the changes in the voltage stability margin and the steady-state overvoltage amplitude before and after optimization in different scenarios.

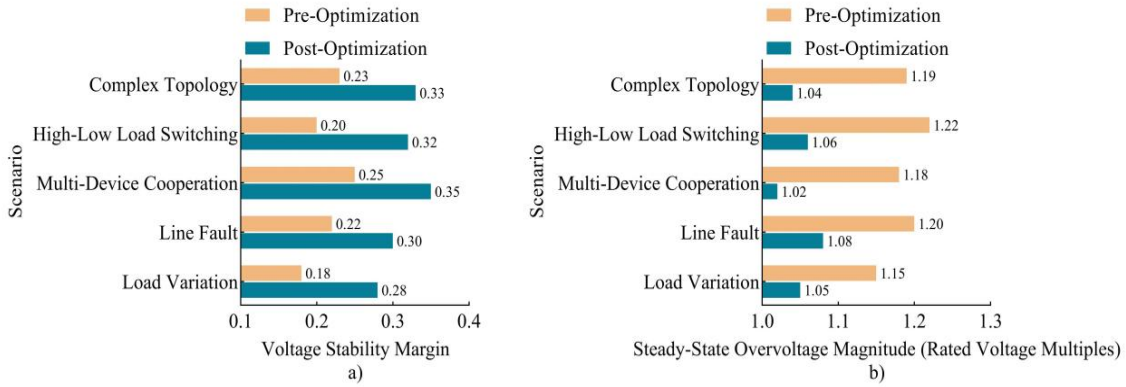


Figure 7. Comparison of voltage stability margin and overvoltage amplitude in different scenarios. (a) Voltage stability margin comparison; (b) Overvoltage amplitude comparison.

The data points in Figure 7 represent the changes in the voltage stability margin and steady-state overvoltage amplitude before and after optimization under different working conditions, respectively, which proves the applicability and optimization effect of the proposed method in various complex environments. In all experimental scenarios, the voltage stability margin of the optimized power grid is significantly improved, while the steady-state overvoltage amplitude is reduced. In the load change scenario, the optimized voltage stability margin is increased from 0.18 to 0.28, and the steady-state overvoltage amplitude is reduced from 1.15 times to 1.05 times, indicating that load fluctuations have a greater impact on the voltage stability of the power grid, and the optimization method can effectively improve the stability of the power grid under load change conditions. In the line fault scenario, the optimization method increases the voltage stability margin from 0.22 to 0.30, and the overvoltage amplitude is reduced from 1.20 times to 1.08 times, indicating that when a fault occurs, the optimization method helps the power grid to recover to a stable state faster. The optimization effect in the multi-equipment collaborative operating scenario and the complex topology scenario is also significant. The change range of the voltage stability margin and the overvoltage amplitude reflects the universal applicability of the optimization method under different topologies and equipment configurations. The optimized power grid shows good adaptability during the switching process between high load and low load. The voltage stability margin increases from 0.20 to 0.32, and the overvoltage amplitude decreases from 1.22 times to 1.06 times. These data show that the optimization method based on IMM can effectively improve voltage stability and reduce the risk of steady-state overvoltage under different power grid conditions.

### *F. Comparative Analysis of IMM and Traditional Voltage Stability Indicators and Effectiveness of GNN Modeling*

IMM and VSM are important indicators for voltage stability evaluation, and their performance under different load conditions is significantly different. Table 4 intuitively shows the evaluation results of the two.

Table 4. Comparative analysis of IMM and VSM under different load conditions.

| Load Condition | IMM Stability Index | VSM Stability Index | Sensitivity Improvement Rate |
|---|---|---|---|
| Light Load | 0.22 | 0.25 | 12% |
| Light-Medium Load | 0.28 | 0.3 | 7% |
| Medium Load | 0.31 | 0.32 | 3% |
| Medium-Heavy Load | 0.36 | 0.32 | 13% |
| Heavy Load | 0.39 | 0.33 | 18% |

The results in Table 4 show that IMM shows high sensitivity under different load conditions, especially in medium and heavy load and heavy load scenarios, where its index value is significantly higher than VSM. This shows that IMM is more suitable for evaluating the voltage stability changes of power grids in complex load scenarios. In addition, the sensitivity improvement rate data also reflects that IMM responds more significantly to load changes.

The modeling method of power grid topology has a direct impact on the accuracy and stability of system analysis. Common modeling methods include those based on graph theory, convolutional neural network (CNN) and recurrent neural network (RNN), which have their own characteristics in different application scenarios. Graph-based methods are suitable for static topological structure analysis, but it is difficult to handle complex dynamic interactions. CNN can extract features using local receptive fields, but its applicability is limited in scenarios with irregular topology. RNN is suitable for time-dependent analysis tasks, but has certain shortcomings in processing global topological information. GNN, because it directly acts on graph structure data, shows strong advantages in capturing nonlinear relationships between nodes and global information propagation. To further verify the performance of different methods in power grid topology modeling, the experiment compared the differences between these methods in terms of modeling complexity, node prediction error, and nonlinear interaction capture ability. The results are shown in Table 5.

Table 5. Performance comparison of GNN and other topology modeling methods.

| Model Type | Modeling Complexity | Nonlinear Interaction Capture Capability | Node Prediction Error (%) | Adaptability to Topological Changes |
|---|---|---|---|---|
| Graph Theory | Low | Weak | 21.5 | Poor |
| CNN | Medium | Moderate | 17.3 | Weak |
| RNN | High | Moderate | 16.8 | Moderate |
| GNN | Medium | Strong | 11.2 | Excellent |

According to the results in Table 5, GNN is superior to other methods in terms of nonlinear interaction capture ability and prediction accuracy. Compared with traditional methods based on graph theory, GNN can use multi-layer information transmission mechanism to model complex associations between nodes more accurately. Compared with CNN and RNN, GNN performs better in topological adaptability, avoiding the problem of CNN being limited by fixed neighborhood structure and RNN losing information when processing topological structure. The comparison results of prediction error further verify this advantage. GNN has the lowest error value, indicating that it is more stable and accurate in power grid data modeling tasks.

## 5. Conclusions

This paper adopts a steady-state overvoltage reactive configuration method for hydropower distribution networks based on the IMM index, and relies on a digital twin simulation model to evaluate voltage stability in real-time. The grid topology and node relationship are extracted through GNN, and the layout and operation strategy of reactive compensation equipment are optimized in combination with the PPO algorithm. In the experiment, this method controls the steady-state overvoltage amplitude at 1.13 times the rated voltage under heavy load conditions, which is significantly lower than the traditional method; under medium and light load conditions, the voltage stability margin is increased to 0.37, and it is still maintained at 0.33 under heavy load conditions; the voltage stability margin of the optimized grid topology reaches 0.38, showing excellent overvoltage control capability. The computational complexity of this method is mainly reflected in three aspects: the digital twin simulation process involves dynamic load and topology adjustment, and the computational complexity is about $O(N^2)$, where N is the number of network nodes; GNN needs to perform multi-layer information aggregation when processing the power grid topology structure, and the computational complexity of each layer is about $O(N^2d)$, where d is the feature dimension, and the overall complexity is affected by the number of layers L to reach $O(LN^2d)$; the PPO algorithm involves policy updates and state space searches in the reinforcement learning optimization process, and the single-step training complexity is O(BC), where B is the batch size, C is the number of policy updates per round of calculation, and the overall complexity is affected by the number of training rounds T to reach O(TBC). In order to reduce the computational complexity, the optimization directions include using sparse matrices to accelerate GNN calculations, parallelizing digital twin simulations to reduce the computational burden, using reinforcement learning strategies based on experience replay to reduce invalid training rounds, and combining dynamic programming methods to reduce the search space of PPO in large-scale scenarios. In the future, the algorithm's computational efficiency can be further optimized and its adaptability to larger-scale power grids can be expanded to better cope with diverse power grid operating conditions and enhance the versatility and practicality of the method. Future work will focus on improving grid security, coordinated optimization control of electric vehicles and grids, and deep integration of renewable energy in distributed power generation systems. The focus will be on studying the impact of electric vehicle charging and discharging strategies on voltage stability, exploring reactive power optimization methods in high-penetration renewable energy environments, and combining advanced control algorithms to improve the stability and reliability of complex grid operations.

## Consent to Publish

The manuscript has not been published before, and it is not being reviewed by any other journal. The authors have all approved the content of the paper.

## Data Availability Statement

The data that support the findings of this study are available from the corresponding author, upon request.

## Conflicts of Interest

The authors affirm that they do not have any financial conflicts of interest.

## References


[1] V.U. Oguanobi, O. Joel. Geoscientific research's influence on renewable energy policies and ecological balancing. Open Access Research Journal of Multidisciplinary Studies, 2024, 7(2), 073-085. DOI: 10.53022/oarjms.2024.7.2.0027

[2] S.F. Stefenon, K.C. Yow, A. Nied, L.H. Meyer. Classification of distribution power grid structures using inception v3 deep neural network. Electrical Engineering, 2022, 104, 4557-4569. DOI: 10.1007/s00202-022-01641-1

[3] P.K. Vishwakarma, M.R. Suyambu. The Impact of Incorporation Renewable Energy on Resilience and Stability of Power Grid System. International Journal of Innovative Science and Research Technology, 2024, 9(10), 1519-1526. DOI: 10.38124/ijisrt/IJISRT24OCT1529

[4] Y.J. Yan, Y.D. Liu, J. Fang, Y.F. Lu, X.C. Jiang. Application status and development trends for intelligent perception of distribution network. High Voltage, 2021, 938-954. DOI: 10.1049/hve2.12159

[5] A. Mishra, T. Manish, P. Ray. A survey on different techniques for distribution network reconfiguration. Journal of Engineering Research, 2023, 173-181. DOI: 10.1016/j.jer.2023.09.001

[6] H. Tian, H.Z. Liu, H. Ma, P.F. Zhang, X.H. Qin, et al. Steady-state voltage-control method considering large-scale wind-power transmission using half-wavelength transmission lines. Global Energy Interconnection, 2021, 4(3), 239-250. DOI: 10.1016/j.gloei.2021.07.009

[7] A. Amanipoor, M.S. Golsorkhi, N. Bayati, M. Savaghebi. V-Iq based control scheme for mitigation of transient overvoltage in distribution feeders with high PV

penetration. IEEE Transactions on Sustainable Energy, 2023, 14(1), 283-296. DOI: 10.1109/TSTE.2022.3211179

[8] S. Xiao, Z.J. Wang, G.N. Wu, Y.J. Guo, G.Q. Gao, et al. The impact analysis of operational overvoltage on traction transformers for high-speed trains based on the improved capacitor network methodology. IEEE Transactions on Transportation Electrification, 2024, 10(1), 364-378. DOI: 10.1109/TTE.2023.3283668

[9] L.X. Cui, D.D. Wang, S.P. Yao, S.M. Wei, H.D. Gao, et al. The Life Cycle Cost Evaluation Model of Typical Power Grid Equipment Asset. Advances in Engineering Technology Research, 2024, 12(1), 363-363. DOI: 10.56028/aetr.12.1.363.2024

[10] N. Li, X.L. Wang, C.Q. Li, W.W. Zhang, Z.J. Zhang. Research on the evaluation method of power grid equipment input–output efficiency based on LCC. Energy Reports, 2023, 9, 1412-1418. DOI: 10.1016/j.egyr.2023.05.212

[11] B. Stone Jr, E. Mallen, M. Rajput, C.J. Gronlund, A.M. Broadbent, et al. Compound climate and infrastructure events: how electrical grid failure alters heat wave risk. Environmental Science & Technology, 2021, 55(10), 6957-6964. DOI: 10.1021/acs.est.1c00024

[12] S. Kumar, A. Pandey, P. Goswami, P. Pentayya, F. Kazi. Analysis of mumbai grid failure restoration on oct 12, 2020: Challenges and lessons learnt. IEEE Transactions on Power Systems, 2022, 37(6), 4555-4567. DOI: 10.1109/TPWRS.2022.3155070

[13] Zhigang, Z. H. A. N. G., and K. A. N. G. Chongqing. Challenges and prospects for constructing the new-type power system towards a carbon neutrality future. Proceedings of the CSEE 42.8 (2022): 2806-2818. DOI: 10.1109/TPWRS.2022.3155070

[14] R.A. Ufa, Y.Y. Malkova, V.E. Rudnik, M.V. Andreev, V.A. Borisov. A review on distributed generation impacts on electric power system. International Journal of Hydrogen Energy, 2022, 47(47), 20347-20361. DOI: 10.1016/j.ijhydene.2022.04.142

[15] P. Ashok, M. Ganesh Madhan. Impedance Characteristics of a Bi-section Gain Lever Laser Diode for 5G Applications. Arabian Journal for Science and Engineering, 2023, 48(6), 8181-8188. DOI: 10.1007/s13369-023-07813-w

[16] C. Kumar, M. Lakshmanan, S. Jaisiva, K. Prabaakaran, S. Barua, et al. Reactive power control in renewable rich power grids: A literature review. IET Renewable Power Generation, 2023, 17(5), 1303-1327. DOI: 10.1049/rpg2.12674

[17] D. Hu, Z.H. Ye, Y.Q. Gao, Z.Z. Ye, Y.G. Peng, et al. Multi-agent deep reinforcement learning for voltage control with coordinated active and reactive power optimization. IEEE Transactions on Smart Grid, 2022, 13(6), 4873-4886. DOI: 10.1109/TSG.2022.3185975

[18] M.A.M. Shaheen, H.M. Hasanien, A. Alkuhayli. A novel hybrid GWO-PSO optimization technique for optimal reactive power dispatch problem solution. Ain Shams Engineering Journal, 2021, 12(1), 621-630. DOI: 10.1016/j.asej.2020.07.011

[19] H. Yapici. Solution of optimal reactive power dispatch problem using pathfinder algorithm. Engineering Optimization, 2021,53(11), 1946-1963. DOI: 10.1080/0305215X.2020.1839443

[20] X.Y. Liang, H. Chai, J. Ravishankar. Analytical methods of voltage stability in renewable dominated power systems: a review. Electricity, 2022, 3(1), 75-107. DOI: 10.3390/electricity3010006

[21] A.R. Nageswa Rao, P. Vijaya, M. Kowsalya. Voltage stability indices for stability assessment: a review. International Journal of Ambient Energy, 2021, 42(7), 829-845. DOI: 10.1080/01430750.2018.1525585

[22] S.S. Kanojia, B.N. Suthar. Voltage stability index: a review based on analytical method, formulation and comparison in renewable dominated power system. International Journal of Applied, 2024, 13(2), 508-520. DOI: 10.11591/ijape.v13.i2.pp508-520

[23] X.Z. Sun, J. Qiu. A customized voltage control strategy for electric vehicles in distribution networks with reinforcement learning method. IEEE Transactions on Industrial Informatics, 2021, 17(10), 6852-6863. DOI: 10.1109/TII.2021.3050039

[24] X.Z. Sun, J. Qiu. Hierarchical voltage control strategy in distribution networks considering customized charging navigation of electric vehicles. IEEE Transactions on Smart Grid, 2021, 12(6), 4752-4764. DOI: 10.1109/TSG.2021.3094891

[25] X.F. Liu, P. Zhang. Adaptive transient overvoltage control strategy for wind farm based on data-driven method. IET Electric Power Applications, 2023, 18(4), 413-424. DOI: 10.1049/elp2.12400

[26] J.R. Chen, M.Y. Liu, F. Milano. Aggregated model of virtual power plants for transient frequency and voltage stability analysis. IEEE Transactions on Power Systems, 2021, 36(5), 4366-4375. DOI: 10.1109/TPWRS.2021.3063280

[27] S. Mokred, Y.F. Wang, T.C. Chen. A novel collapse prediction index for voltage stability analysis and contingency ranking in power systems. Protection and Control of Modern Power Systems, 2023, 8(1), 1-27. DOI: 10.1186/s41601-023-00279-w

[28] S. Omi, Y. Shirai. Robust calculation method of voltage stability margin based on voltage-collapse-point properties. IEEJ Transactions on Electrical and Electronic Engineering, 2021, 16(11), 1463-1469. DOI: 10.1002/tee.23449

[29] A.M.S. Alonso, L.D.O. Arenas, D.I. Brandao, E. Tedeschi, F.P. Marafao. Integrated local and coordinated overvoltage control to increase energy feed-in and expand DER participation in low-voltage networks. IEEE Transactions on Sustainable Energy, 2022, 13(2), 1049-1061. DOI: 10.1109/TSTE.2022.3146196

[30] Z.H.A.N.G. Yuanyuan, H.A.N. Bin, Q.I.N. Xiaohui, Y.I.X.I. Cuomu, L.I. Suning, et al. Overvoltage Mechanism, Properties and Restriction Requirements of AC Half-wave Length Transmission System. Power System Technology, 2022, 47(6), 2452-2462. DOI: 10.13335/j.1000-3673.pst.2022.1636

[31] A. Eid, S. Kamel, L. Abualigah. Marine predators algorithm for optimal allocation of active and reactive power resources in distribution networks. Neural Computing and Applications, 2021, 33(21), 14327-14355. DOI: 10.1007/s00521-021-06078-4

[32] M.K. Kar, S. Kumar, A.K. Singh, S. Panigrahi. Reactive power management by using a modified differential evolution algorithm. Optimal Control Applications and Methods, 2023, 44(2), 967-986. DOI: 10.1002/oca.2815

[33] L. Kumar, M.K. Kar, S. Kumar. Reactive power management of transmission network using evolutionary techniques. Journal of Electrical Engineering & Technology, 2023, 18(1), 123-145. DOI: 10.1007/s42835-022-01185-1

[34] F.J. Hao, G. Zhang, J. Chen, Z.G. Liu. Distributed reactive power compensation method in DC traction power systems with reversible substations. IEEE Transactions on Vehicular Technology, 2021, 70(10), 9935-9944. DOI: 10.1109/TVT.2021.3108030

[35] M. Tofighi-Milani, S. Fattaheian-Dehkordi, M. Fotuhi-Firuzabad, M. Lehtonen. Distributed reactive power management in multi-agent energy systems considering voltage profile improvement. IET Generation, Transmission & Distribution, 2023, 17(21), 4891-4906.

DOI: 10.1049/gtd2.13005
[36] Y.Q. Ji, X.H. Chen, T. Wang, P. He, N. Jin, et al. Dynamic reactive power optimization of distribution network with distributed generation based on fuzzy time clustering. IET Generation, Transmission & Distribution, 2021, 16(7), 1349-1363. DOI: 10.1049/gtd2.12370
[37] A.S. Alayande, I.K. Okakwu, O.E. Olabode, C.C. Ike, A.A. Makinde. Estimation and Allocation of Reactive Power Loss in Interconnected Power Systems Through Network Structural Characteristics Theory. Arabian Journal for Science and Engineering, 2020, 46(2), 1225-1239. DOI: 10.1007/s13369-020-04944-2
[38] M.H. Hassan, S. Kamel, M.A. El-Dabah, T. Khurshaid, J.L. Dominguez-Garcia. Optimal reactive power dispatch with time-varying demand and renewable energy uncertainty using Rao-3 algorithm. IEEE Access, 2021, 9, 23264-23283. DOI: 10.1109/ACCESS.2021.3056423
[39] G.U.O. Ting, C.H.E.N. Zhonghao, X.U. Liangde, Y.A.N.G Fan. Research on the Two-stage Multi-objective Optimal Configuration Method of Reactive Power Compensation Devices in Power Grid Based on Power Loss Index. Journal of Electrical Engineering, 2024, 18(4), 239-250. DOI: 10.11985/2023.04.026